MEMORANDUM
RM-5379-NASA
AUGUST 1967

TRANSIONOSPHERIC PROPAGATION OF FM SIGNALS

E. Bedrosian

This research is sponsored by the National Aeronautics and Space Administration under Contract No. NASr-21. This report does not necessarily represent the views of the National Aeronautics and Space Administration.

The RAND Corporation
1700 MAIN ST. • SANTA MONICA • CALIFORNIA • 90406

Published by The RAND Corporation

RAND RESEARCH
BRIEF
THE RAND CORPORATION
1700 Main St. · Santa Monica · California · 90406

August 1967 RB-5379

RM-5379-NASA, Transionospheric Propagation of FM Signals, E. Bedrosian, RAND Memorandum, August 1967, 50 pp.

PURPOSE: To examine and compute the distortion experienced by a wide-band frequency-modulated (or phase-modulated) signal as it is transmitted through the earth's ionosphere. The results can be used as an aid in designing satellite systems that transmit television or multichannel telephone signals.

RELATED TO: RAND's continuing study of communication satellite technology for the National Aeronautics and Space Administration.

DISCUSSION AND METHODOLOGY: When a terrestrial station is linked to an earth satellite at synchronous altitude, the propagation path traverses virtually the entire ionosphere in a direction depending on the relative location of the station and the satellite. This path can range from the zenith to the near horizon. The average integrated electron density through the ionosphere is about 10^{17} electrons/m^2, but can vary by a factor of 10. Efficient use of satellite power requires wide-band transmissions, and distortion of signal occurs because of the dispersive effects of the ionosphere, with greater effects at lower carrier frequencies and during periods of solar activity. Previous work has been concerned with the transmission of individual pulses, and with spectral analyses for wide-band FM, based on expanding the quasi-stationary approximation to the filtering effect of the ionosphere and retaining the lower-order distortion terms. The present analysis used a modification of the Bedrosian-Rice technique (P-3502, Distortion and Cross-talk of Linearly Filtered, Angle-modulated Signals, March 1967). An expansion was obtained for the phase of an angle-modulated (AM) signal passed through a general linear filter, and a spectral analysis was performed. The ionosphere was then modeled as such a filter, and numerical computations of the output linear-signal, cross-power, and intermodulation spectra were performed for the case of an FM signal having a flat gaussian baseband. Two examples of current interest were examined numerically: a high-capacity communication link of the Intelsat type, and a wide-band video transmission near the upper end of the UHF television band.

PRINCIPAL FINDINGS: Ionospheric dispersion will not cause significant intermodulation distortion in a typical wide-band FM communication satellite link except under the most severe conditions. Nevertheless, for a given baseband signal and r-f bandwidth, operation over a given path should be at as high a carrier frequency as possible.

The situation is less promising with respect to color television. The calculated ratios of signal-to-distortion and to cross-talk are about 20 db. It is difficult to assess the subjective effect of intermodulation distortion for a hypothetical TV distribution system using wide-band FM transmission from a satellite relay as compared with the "snow" produced by a conventional vestigial-sideband AM transmission corrupted by thermal noise. The thermal noise in AM video is uniform, whereas the intermodulation distortion of FM varies roughly as the square of the baseband frequency and can display a strong correlation with the signal. Color transmission would suffer also from a degradation of color separation because of synchronizing phase errors. Just how objectionable these effects would be cannot be determined by computation. An experimental investigation would be desirable.

MW

PREFACE

This study, undertaken as part of RAND's continuing study of Communications Satellite Technology for the National Aeronautics and Space Administration, considers the intermodulation, or distortion, experienced by a wide-band, frequency-modulated signal as it is transmitted through the earth's ionosphere.

The efficient use of the power available from satellites requires the use of wide-band transmission. Distortion occurs because of the dispersive effects of the earth's ionosphere, with the effects greater at the lower carrier frequencies and during periods of solar activity. This Memorandum studies this phenomenon and provides a means for computing the resulting distortion. The results of the study can be used as an aid for designing satellite systems that transmit television or multichannel telephone signals.

SUMMARY

Communication links to earth satellites are not usually affected adversely in traversing the ionosphere. However, the nonlinear variation of the refractive index with frequency causes a dispersion which can result in significant signal distortion under certain circumstances. A wide-band signal operating at the lower carrier frequencies and taking a low-elevation path through a disturbed ionosphere constitutes such a case. The effect of ionospheric dispersion is examined in this Memorandum for the particular case of frequency (or phase) modulation.

In a previous analysis (P-3502, Distortion and Crosstalk of Linearly Filtered, Angle-modulated Signals, The RAND Corporation, by E. Bedrosian and S. O. Rice) an expansion was developed for the output phase of an angle-modulated signal which had been passed through a generalized linear filter. The ionosphere is modeled as such a filter in this Memorandum, and a spectral analysis of the demodulated signal is performed assuming a gaussian modulating waveform. From this, formulas are obtained for the output signal-to-distortion and signal-to-cross-talk ratios. All of the spectral results are presented graphically for FM with a uniform baseband.

Two cases of current interest are examined numerically to illustrate the use of the results. The first case typifies a high-capacity communication link of the Intelsat variety, and it is seen that a significant degradation can occur only under the most unusual conditions. The second example considers a wide-band TV transmission near the upper end of the UHF TV band; in this case, ratios of signal-to-distortion and to cross-talk of about 20 db result. Ratios of this

order are clearly cause for concern, but it is not possible to assess their subjective effect by relating them to the familiar interference produced by thermal noise which is uncorrelated with the signal. Also, a TV signal, particularly if color, is not as well modeled by a gaussian signal as is a typical multichannel telephone baseband. For these reasons, it is concluded that an experimental investigation would be desirable both to verify the theory and to develop subjective interference criteria.

CONTENTS

LIST OF FIGURES

I. INTRODUCTION

Communication links between terrestrial stations and earth satellites or space probes invariably employ operating frequencies well above those for which ionospheric absorption or refraction are significant. Other effects, such as Faraday rotation and path splitting, are either found to be unimportant or are accommodated without difficulty. However, this is not necessarily the case for the dispersion produced by the nonlinear variation of the velocity of propagation with frequency. A wide-band signal traversing a disturbed ionosphere can experience considerable distortion at the lower carrier frequencies.

Much of the work to date on ionospheric-induced distortion has been concerned with the transmission of individual pulses or of pulse-type modulation, although some attention has also been directed to analog-type modulation. This work is briefly reviewed in Ref. 1. The earliest work which appears to relate directly to the results presented here was done by Rice[2] in 1957. He approximates the expression for the output phase of a filtered signal for the case of small distortion and then performs a spectral analysis using second-order modulation terms. In particular, he obtains the spectrum of the "interchannel interference" (Eq. (5.5)) when an FM signal having a flat gaussian baseband is passed through a filter with a uniform attenuation and quadratic phase characteristic. It will be shown later in this study that this yields a narrow-band approximation to the more precise result presented here.

Direct applications to ionospheric propagation of wide-band FM, which is of interest in broadcasting and relaying TV signals, were performed by Shaft,[3] and Prosin[4] in 1963, and by Denton, Scheibe and

Huntsberger[5] in 1965 using the quasistationary approximation to the filtering effect of the ionosphere. In each case, the distortion spectrum (Shaft, Eq. (21); Prosin, Eq. (39); Denton, et al., Eq. (4.26)) is obtained by expanding the quasistationary approximation and retaining the lower order distortion terms, thereby yielding results which agree with Rice's approximation given in Ref. 2.

The following analysis is based on the technique described by Bedrosian and Rice[6] wherein an expansion is obtained for the phase of an angle-modulated signal passed through a general linear filter. The expansion is then specialized to the case of a symmetrical band-pass filter, and the output spectrum is computed numerically for the case when an FM signal, having a flat gaussian baseband, is passed through a single-pole filter.

In this Memorandum, a spectral analysis is performed when a general filter is used. The ionosphere is then modeled as such a filter and numerical computations of the output spectrum are again performed for the case of an FM signal having a flat gaussian baseband. The results are interpreted for specific examples of transionospheric propagation of a wide-band FM signal using communication and video basebands. The signal-to-distortion ratios predicted in a TV case of potential interest are shown to be poor enough in comparison with the accepted signal-to-noise criteria for high-fidelity transmission to warrant an experimental investigation to determine the nature and subjective effect of distortion.

II. OUTPUT PHASE FUNCTION

Consider the angle-modulated signal

$$s(t) = \exp i[2\pi f_o t + \varphi(t)] \tag{1}$$

where f_o is the carrier frequency and φ is the modulating signal. When this signal is passed through a filter having an impulse response, g, and a transfer function, G, where

$$G(f) = \int_{-\infty}^{\infty} g(t)e^{-i2\pi ft}\,dt, \quad g(t) = \int_{-\infty}^{\infty} G(f)e^{i2\pi ft}\,df \tag{2}$$

are a Fourier pair, then the output phase, θ, is given by[6]

$$\theta(t) = -\beta_o + \text{Re}\ \Phi(t) + \sum_{n=2}^{\infty} \frac{1}{n!}\ \text{Im}\ i^n f_n \tag{3}$$

where β_o is the phase shift at the carrier frequency

$$\beta_o = -\text{Im}\ \log\ G(f_o) \tag{4}$$

and the function Φ is given by

$$\Phi(t) = \int_0^{\infty} \gamma(\tau)\varphi(t-\tau)d\tau \tag{5}$$

where

$$\gamma(t) = \frac{g(t)e^{-i2\pi f_o t}}{G(f_o)} \tag{6}$$

The first four coefficients in the series are

$$\begin{aligned} f_2 &= F_2, & f_4 &= F_4 - 3\,F_2^2 \\ f_3 &= F_3, & f_5 &= F_5 - 10\,F_3\,F_2 \end{aligned} \tag{7}$$

where

$$F_n = \int_0^\infty \gamma(\tau)[\varphi(t-\tau)-\Phi(t)]^n \, d\tau \tag{8}$$

Additional coefficients and a discussion of the convergence of this series are presented in Ref. 6.

The impulse response, γ, given by Eq. (6) is associated with a filter which is a normalized, frequency-shifted version of the original filter. The transfer function of this hypothetical filter is

$$\Gamma(f) = \frac{G(f+f_o)}{G(f_o)} \tag{9}$$

and it follows, from Eqs. (2) and (6), that

$$\int_0^\infty \gamma(\tau)d\tau = \Gamma(0) = 1 \tag{10}$$

If the original filter is physically realizable, then its impulse response, g, vanishes for $t < 0$ and is real, while its transfer function, G, has an even real part and an odd imaginary part by virtue of Eq. (2). From Eq. (6), it is seen that the impulse response, γ, of the normalized frequency-shifted filter also vanishes for $t < 0$, but γ is complex in general, and its associated transfer function, Γ, lacks the symmetry properties of G.

It is convenient, therefore, to write

$$\gamma(t) = \gamma_r(t) + i\,\gamma_i(t) \tag{11}$$

where, from Eq. (10),

$$\int_0^\infty \gamma_r(t)dt = 1, \qquad \int_0^\infty \gamma_i(t)dt = 0 \tag{12}$$

Then, since γ_r and γ_i are real functions, it follows that they can be associated with the transfer functions

$$\Delta(f) = \int_0^\infty \gamma_r(t) e^{-i2\pi ft}\, dt$$

$$\Lambda(f) = \int_0^\infty \gamma_i(t) e^{-i2\pi ft}\, dt \tag{13}$$

which do have the even real-part and odd imaginary-part symmetry of G. Of course, Δ and Λ are complex, in general. In terms of the real and imaginary parts of Γ,

$$\Gamma(f) = \Gamma_r(f) + i\Gamma_i(f) = \Delta(f) + i\Lambda(f) \tag{14}$$

from which it is seen that

$$\Delta(f) = \frac{1}{2}\left[\Gamma_r(f)+\Gamma_r(-f)\right] + i\,\frac{1}{2}\left[\Gamma_i(f)-\Gamma_i(-f)\right]$$

$$\Lambda(f) = \frac{1}{2}\left[\Gamma_i(f)+\Gamma_i(-f)\right] - i\,\frac{1}{2}\left[\Gamma_r(f)-\Gamma_r(-f)\right] \tag{15}$$

These functions completely characterize the normalized, frequency-shifted filter to be used in the ensuing spectral analysis.

The output phase through terms of third order is, from Eq. (3),

$$\theta(t) = -\beta_o + \mathrm{Re}\,\Phi(t) + \frac{1}{2!}\,\mathrm{Im}\,i^2 f_2 + \frac{1}{3!}\,\mathrm{Im}\,i^3 f_3 + \ldots \tag{16}$$

Writing the function Φ in terms of its real and imaginary parts yields

$$\Phi(t) = \Phi_r(t) + i\,\Phi_i(t)$$

$$= \int_0^\infty \gamma_r(\tau)\varphi(t-\tau)\,d\tau + i\int_0^\infty \gamma_i(\tau)\varphi(t-\tau)\,d\tau \tag{17}$$

Substituting in Eqs. (7) and (8) and noting Eqs. (12) then leads to

$$\theta(t) = -\beta_o + \Phi_r(t) - \frac{1}{2}\int_0^\infty \gamma_i(\tau)\left[\varphi(t-\tau)-\Phi_r(t)\right]^2 d\tau$$

$$- \frac{1}{6}\int_0^\infty \gamma_r(\tau)\left[\varphi(t-\tau)-\Phi_r(t)\right]^3 d\tau$$

$$- \frac{1}{2}\Phi_i(t)\int_0^\infty \gamma_i(\tau)\left[\varphi(t-\tau)-\Phi_r(t)\right]^2 d\tau + \ldots \qquad (18)$$

which is the desired form of the output phase. The leading term yields the basic phase shift at the carrier frequency. Depending on the nature of the input phase, φ, additional phase shifts will, in general, be contributed by the remaining terms. Even if φ is zero mean, phase shifts can be generated by terms such as the third one.

The second term in Eq. (18) is a linearly filtered version of the input and represents the principal time-varying component of the output when the distortion is small. Successive terms yield the various orders of distortion to the output.

III. SPECTRAL ANALYSIS

The spectral density, W_θ, of the output phase, θ, will be determined by the conventional technique of taking the Fourier transform of the autocorrelation function of θ

$$W_\theta(f) = \mathfrak{F}\, E\, \theta(t)\theta(t-\tau) \tag{19}$$

where $\mathfrak{F}$ denotes the Fourier transform operator and E, the expectation operator, denotes an ensemble average defining the autocorrelation function

$$R_\theta(\tau) = E\, \theta(t)\theta(t+\tau) \tag{20}$$

and where R and W are a Fourier pair. In terms of phase rates

$$W_{\dot\theta}(f) = (2\pi f)^2 W_\theta(f); \qquad W_\varphi(f) = W_{\dot\varphi}(f)/(2\pi f)^2 \tag{21}$$

If angles are measured in radians and frequency in hertz, the units of W_θ are rad^2/Hz, and those of $W_{\dot\theta}$ are $(rad/s)^2/Hz$.

When the expansion for the output phase given by Eq. (18) is substituted in Eq. (19), the results contain a variety of functional pairings. Let β, Φ, f_2, f_3, etc., denote the terms in the output phase given by Eq. (18) and denote the individual pairings by terms such as

$$\Phi \times f = \mathfrak{F}\, E\, \Phi(t) f(t+\tau) \tag{22}$$

Then, as discussed in Ref. 6, the "linear-signal" component of the output spectrum is identified as the $\Phi\times\Phi$ term and denoted by W_θ^L. The $\Phi\times f$ and $f\times f$ terms contribute some output spectral components in which the input spectrum, W_φ, appears as a multiplier; these are identified as the "cross-power" component of the output spectrum and are denoted by W_θ^C. The "intermodulation" component of the output spectrum is denoted

by W_θ^I and is given by the balance of the frequency-dependent spectral terms which result from the f×f pairings. In addition to these three types, which are identified in Ref. 6, a zero-frequency or "dc" term, denoted by $\overline{\theta^2}$, appears in the analysis of the general case.

For the purposes of the spectral analysis, the input signal, φ, is taken as a gaussian process having a spectral density, W_φ (the details of the analysis are presented in the Appendix). The leading terms of the various components of the output spectral density are given by

$$\overline{\theta^2} = \beta_o^2 - 2\beta_o \int_{-\infty}^{\infty} d\rho \; W_\varphi(\rho) \mathrm{Re}\; \Delta(\rho)\Lambda(-\rho)$$

$$W_\theta^L(f) = |\Delta(f)|^2 W_\varphi(f)$$

$$W_\theta^C(f) = 2W_\varphi(f) \int_{-\infty}^{\infty} d\rho \; W_\varphi(\rho)\{\mathrm{Re}\; \Delta(f)[\Delta(\rho)\Delta(-\rho-f)-\Lambda(\rho)\Lambda(-\rho-f)]$$

$$+ |\Delta(f)|^2[|\Lambda(\rho)|^2-|\Delta(\rho)|]^2 + 2\mathrm{Re}\; \Delta(f)\Lambda(-f)\Delta(\rho)\Lambda(-\rho)\}$$

$$W_\theta^I(f) = \frac{1}{2} \int_{-\infty}^{\infty} d\rho \; W_\varphi(\rho)W_\varphi(f-\rho)\,|\Delta(\rho)\Lambda(f-\rho) + \Lambda(\rho)\Delta(f-\rho) - \Lambda(f)|^2 \qquad (23)$$

The principal dc term results from the $\beta\times\beta$ operation with a second-order correction from the $\beta\times f_2$ term; third-order corrections, which are not shown, come from the $\beta\times f_4$ and $f_2\times f_2$ terms. As stated above, the linear-signal component is due to the $\Phi\times\Phi$ term. The cross-power component is due solely to the $\Phi\times f_3$ term since the $f_2\times f_2$ term yields only an intermodulation component in this case.

IV. APPLICATION TO IONOSPHERE

A transfer function which is characteristic of the transionospheric propagation path is required to use the foregoing analysis. Since, for all practical purposes, the ionosphere behaves as a linear medium and is time-invariant on time scales of interest for communication purposes, it follows that the propagation path under consideration can be modeled as a cascade of the same path in vacuo and a filter which reflects only the properties of the ionosphere. The transfer function of that filter is then given by the ratio of the steady-state frequency response of the actual transionospheric path to that of the free-space path.

The relative bandwidth of the transmitted signal will be assumed to be sufficiently small, and the carrier frequency sufficiently large in comparison with the plasma frequency, so that the effect of ionospheric absorption can be neglected. Since the distance dependence is the same for both paths, it follows that the transfer function depends solely on the difference between the phase characteristics of the two paths, and is given by

$$G(f) = \exp\left[ik \int (n-1)ds\right] \tag{24}$$

where

$k = 2\pi f/c$ is the phase constant

$c = 3 \times 10^8$ m/s is the speed of light

$n = \left(1-f_p^2/f^2\right)^{\frac{1}{2}}$ is the refractive index of the ionosphere at frequencies well above the plasma frequency, f_p, and the integration is along the propagation path.

For frequencies large in comparison with the plasma frequency, the refractive index can be expanded in a binomial series. Then, expanding the leading term, $1/f$, in a Taylor's series about the carrier frequency, f_o, yields the high-frequency narrow-band approximation

$$G(f) = \exp\left\{ i \frac{\pi}{c} \left[\frac{1}{f_o} - \frac{f - f_o}{f_o^2} + \frac{(f-f_o)^2}{f_o^3} \right] \int f_p^2 \, ds \right\} \tag{25}$$

where the various terms represent, respectively, the constant, linear and quadratic components of the frequency-dependent phase shift introduced by the ionosphere. To simplify the expression, let

$$f_c^2 = \frac{c f_o^3}{\pi \int f_p^2 \, ds}. \tag{26}$$

Then, denoting normalization to f_c by underlining yields

$$\beta_o = -\mathrm{Im} \log G(f_o) = -\underline{f}_o^2 , \qquad \underline{f}_o = \frac{f_o}{f_c} \tag{27}$$

for the carrier-frequency phase shift, β_o, defined by Eq. (4). The transfer function, Γ, of the normalized, frequency-shifted equivalent filter of the ionosphere then becomes, from Eq. (9),

$$\Gamma(f) = \frac{G(f+f_o)}{G(f_o)} = \exp(-i\underline{f}_o \underline{f} + i\underline{f}^2), \qquad \underline{f} = \frac{f}{f_c} \tag{28}$$

and the associated transfer functions defined by Eq. (15) become

$$\Delta(f) = e^{-i\underline{f}_o \underline{f}} \cos \underline{f}^2, \qquad \Lambda(f) = e^{-i\underline{f}_o \underline{f}} \sin \underline{f}^2 \tag{29}$$

When these functions are substituted into the expressions for the components of the output spectral density given by Eq. (23), the result is

$$\overline{\theta^2} = \underline{f}_o^4 + \underline{f}_o^2 \int_{-\infty}^{\infty} d\rho \; W_\varphi(\rho) \sin 2\underline{\rho}^2$$

$$W_\theta^L(f) = W_\varphi(f) \cos^2 \underline{f}^2$$

$$W_\theta^C(f) = -4 \cos \underline{f}^2 \; W_\varphi(f) \int_{-\infty}^{\infty} d\rho \; W_\varphi(\rho) \cos(\underline{f}^2 + 2\underline{\rho}^2) \sin^2 \underline{\rho f}$$

$$W_\theta^I(f) = 2 \int_{-\infty}^{\infty} d\rho \; W_\varphi(\rho) W_\varphi(f-\rho) \sin^2 \underline{\rho}(\underline{\rho} - \underline{f}) \cos^2(\underline{\rho}^2 - \underline{\rho f} + \underline{f}^2) \tag{30}$$

It is not surprising that the terms in $\underline{f}$ appearing in Δ and Λ vanish in the expressions for the output spectrum, since a term which is linear in frequency can be expected to yield only a pure time delay to the propagated signal.

The parameter, f_c, has the units of frequency, and can be seen from Eq. (28) to correspond to that frequency difference from the carrier frequency at which the square-law component of the nonlinear phase shift produced by the ionosphere equals one radian. Thus, it serves as a convenient measure of the degree of nonlinearity in the phase characteristic of the ionosphere. Since there is no need to consider an accompanying nonlinear amplitude characteristic, f_c will be referred to simply as the "characteristic frequency" of the ionosphere at that carrier frequency.

For computational purposes, it is more convenient to express the characteristic frequency in terms of the electron density rather than the plasma frequency. As is well known[7]

$$\omega_P^2 = \frac{e^2 N_e}{\epsilon_o m}, \qquad \omega_P = 2\pi f_p \tag{31}$$

where

$e = 1.602 \times 10^{-19}$ C is the electron charge

$m = 9.109 \times 10^{-31}$ kg is the electron mass

$\epsilon_o = 8.854 \times 10^{-12}$ F/m is the permittivity of free space

N_e = electron density in electrons/m^3

Substituting in Eq. (26) and defining

$$N_T = \int N_e \, ds, \qquad \text{electrons/m}^2 \tag{32}$$

as the electron density integrated along the propagation path then yields

$$f_c = 1.088 \times 10^3 \frac{f_o^{3/2}}{N_T^{1/2}}, \quad \text{Hz} \tag{33}$$

where f_o is the carrier frequency in Hz. The characteristic frequency is plotted as a function of carrier frequency for a number of integrated electron densities in Fig. 1.

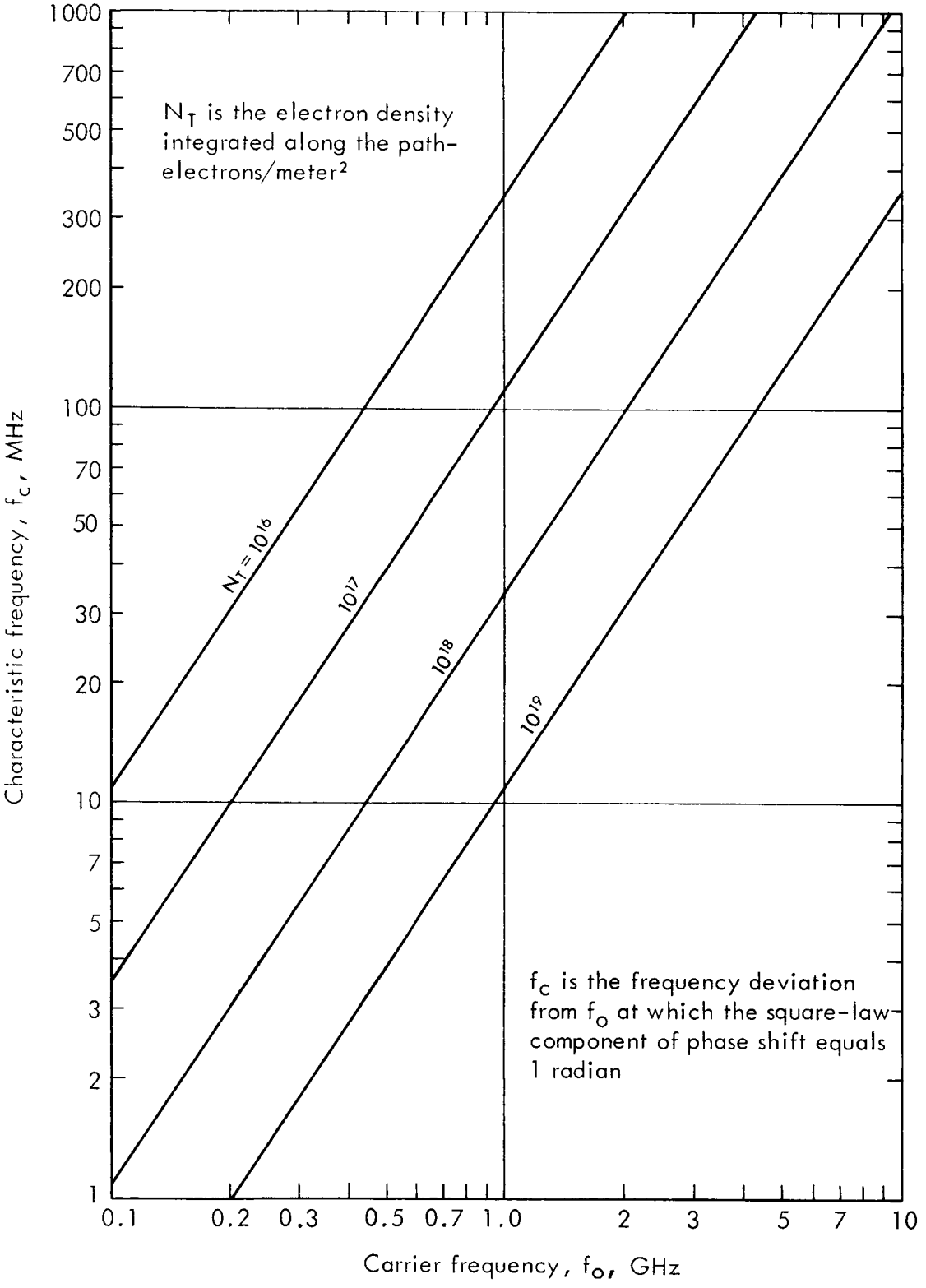

Fig. 1 — Characteristic frequency of the ionosphere

V. COMPUTATIONS FOR FM WITH A UNIFORM BASEBAND

One transmitted signal of practical interest is that generated by using a gaussian baseband signal, with a spectral density uniform in (-B,B) and zero elsewhere, to frequency modulate a carrier at an rms frequency deviation, D. Such a baseband signal closely approximates a multichannel, frequency-division-multiplexed telephone signal. It also approximates a television video signal, though less well, partly because typical video spectra are not uniform and partly because the amplitude distribution of a video signal is less nearly gaussian than that of a multichannel telephone signal.*

The spectral density of the input phase rate will therefore be taken as

$$W_{\dot{\varphi}}(f) = \frac{2\pi^2 D^2}{B} , \qquad |f| \leq B \tag{34}$$

and zero elsewhere. Then, using Eqs. (21) to convert between the spectra of phases and phase rates and substituting Eq. (34) into Eqs. (30) yields the following spectral components of the output phase rate

*Other related properties are discussed in the next section.

$$\frac{W_{\dot{\theta}}^{L}(f)}{D^2/f_c} = \frac{2\pi^2}{\underline{B}} \cos^2 \underline{f}^2 , \qquad |f| \le B$$

$$\frac{W_{\dot{\theta}}^{C}(f)}{D^4/f_c^3} = -\frac{8\pi^2}{B^2} \cos \underline{f}^2 \int_0^{\underline{B}} \frac{d\underline{\rho}}{\underline{\rho}^2} \cos(\underline{f}^2+2\underline{\rho}^2) \sin^2 \underline{\rho f} , \qquad |f| \le B$$

$$\frac{W_{\dot{\theta}}^{I}(f)}{D^4/f_c^3} = \frac{2\pi^2 \underline{f}^2}{\underline{B}^2} \int_{|\underline{f}|-\underline{B}}^{\underline{B}} \frac{d\underline{\rho}}{\underline{\rho}^2(\underline{\rho}-|\underline{f}|)^2}$$

$$\times \sin^2 \underline{\rho}(\underline{\rho}-|\underline{f}|) \cos^2(\underline{\rho}^2-\underline{\rho}|\underline{f}|+\underline{f}^2) , \qquad |f| \le 2B \qquad (35)$$

where it is understood that the terms vanish in those frequency intervals in which they are not defined and where underlining indicates normalization to f_c.

The spectral density of the linear-signal component of the output phase rate given by the first of Eqs. (35) is plotted as a function of the relative baseband frequency, f/B, for a number of normalized baseband frequencies, B/f_c, in Figs. 2 and 3.* A feature of note is the progressive drop in the high-frequency content as the baseband is widened relative to the characteristic frequency.

The magnitude of the cross-power spectral density given by the second of Eqs. (35) is plotted in a similar fashion in Figs. 4 and 5. Unlike the linear-signal component which results from a pure autocorrelation and therefore has a real, positive, even spectral density,

*These and all subsequent computations were performed numerically using the RAND JOSS computer. JOSS is the trademark and service mark of The RAND Corporation for its on-line time-shared computer program and services using that program.

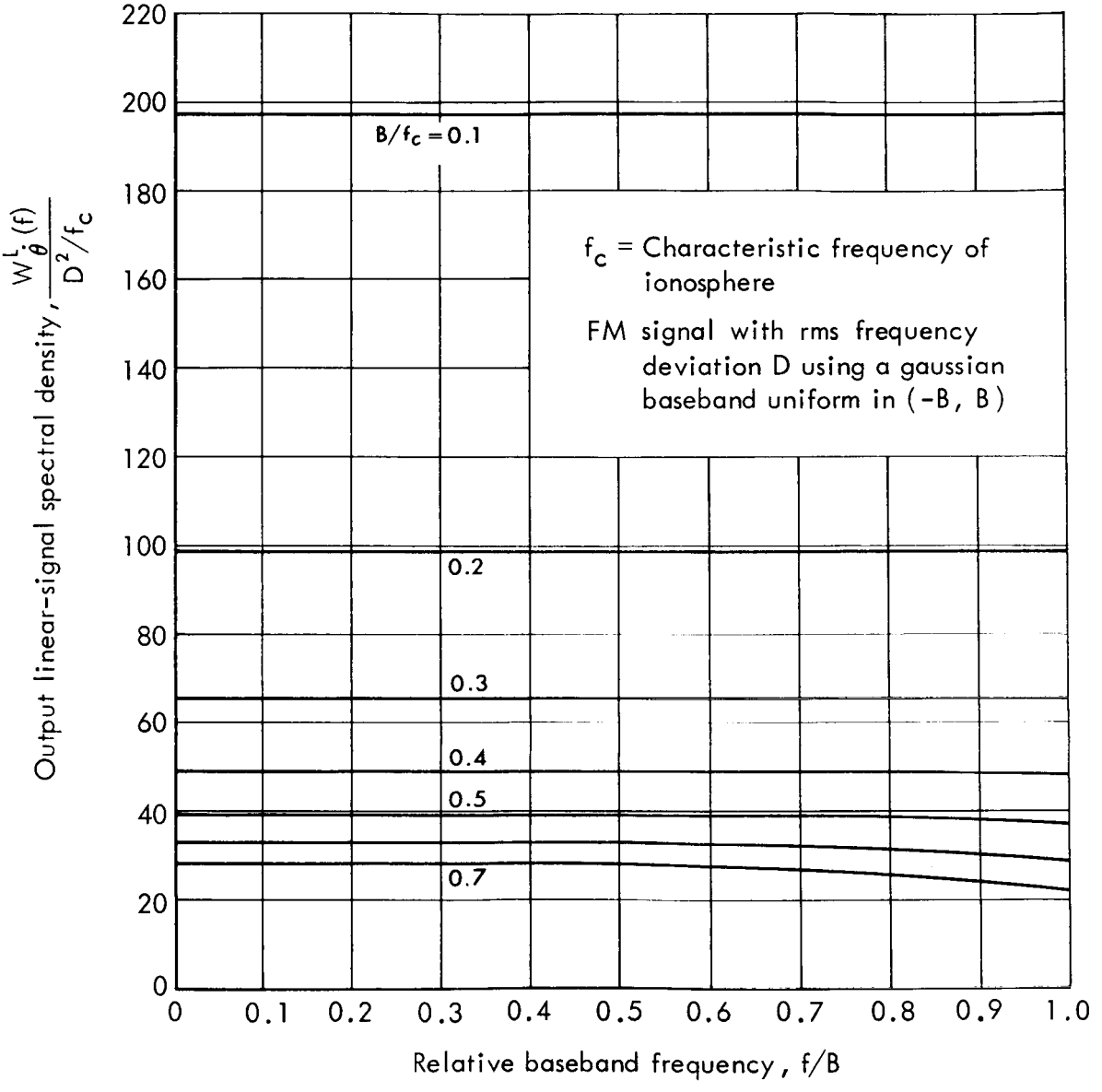

Fig. 2 — Output linear-signal spectral density

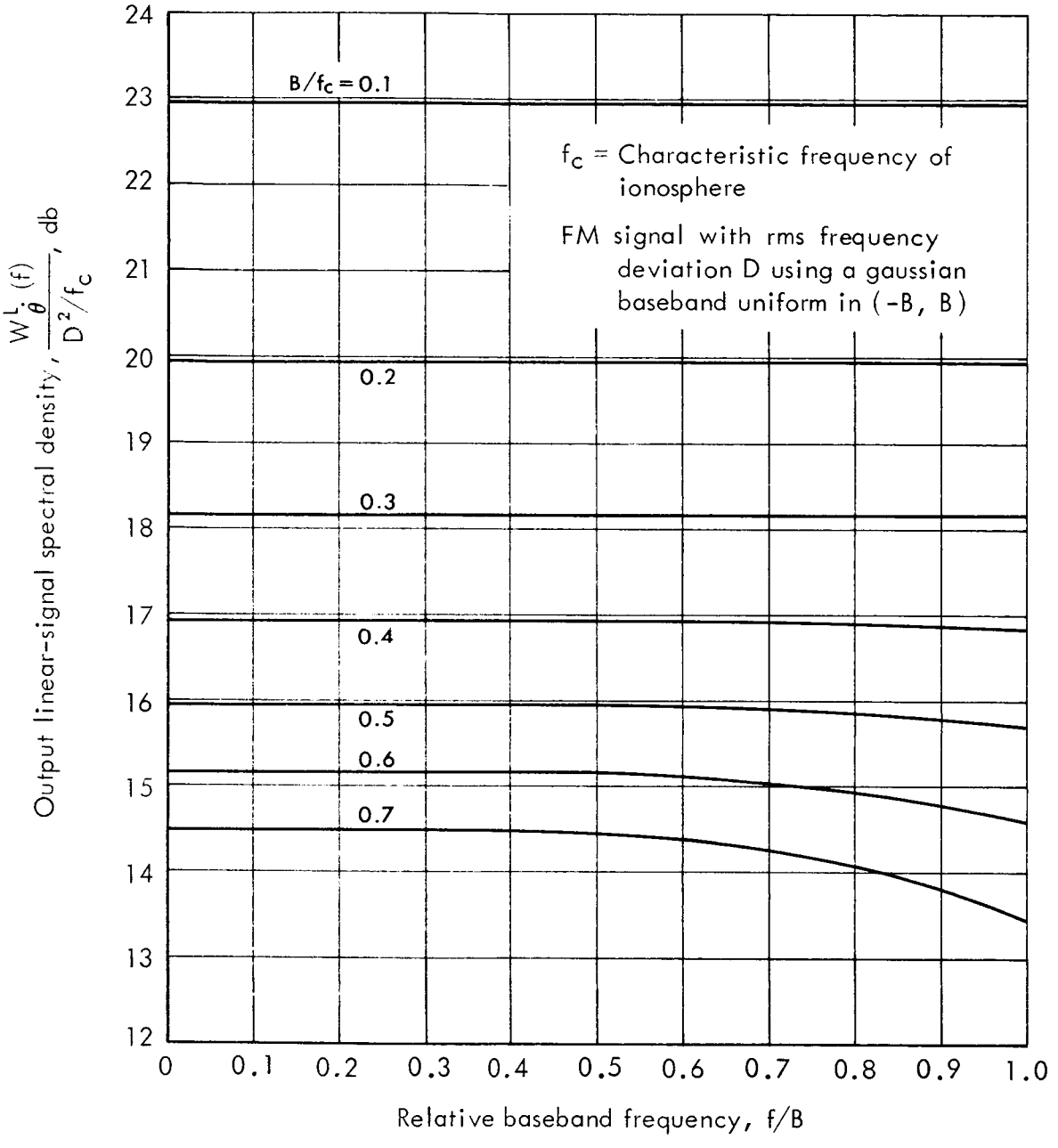

Fig. 3 — Output linear-signal spectral density, db

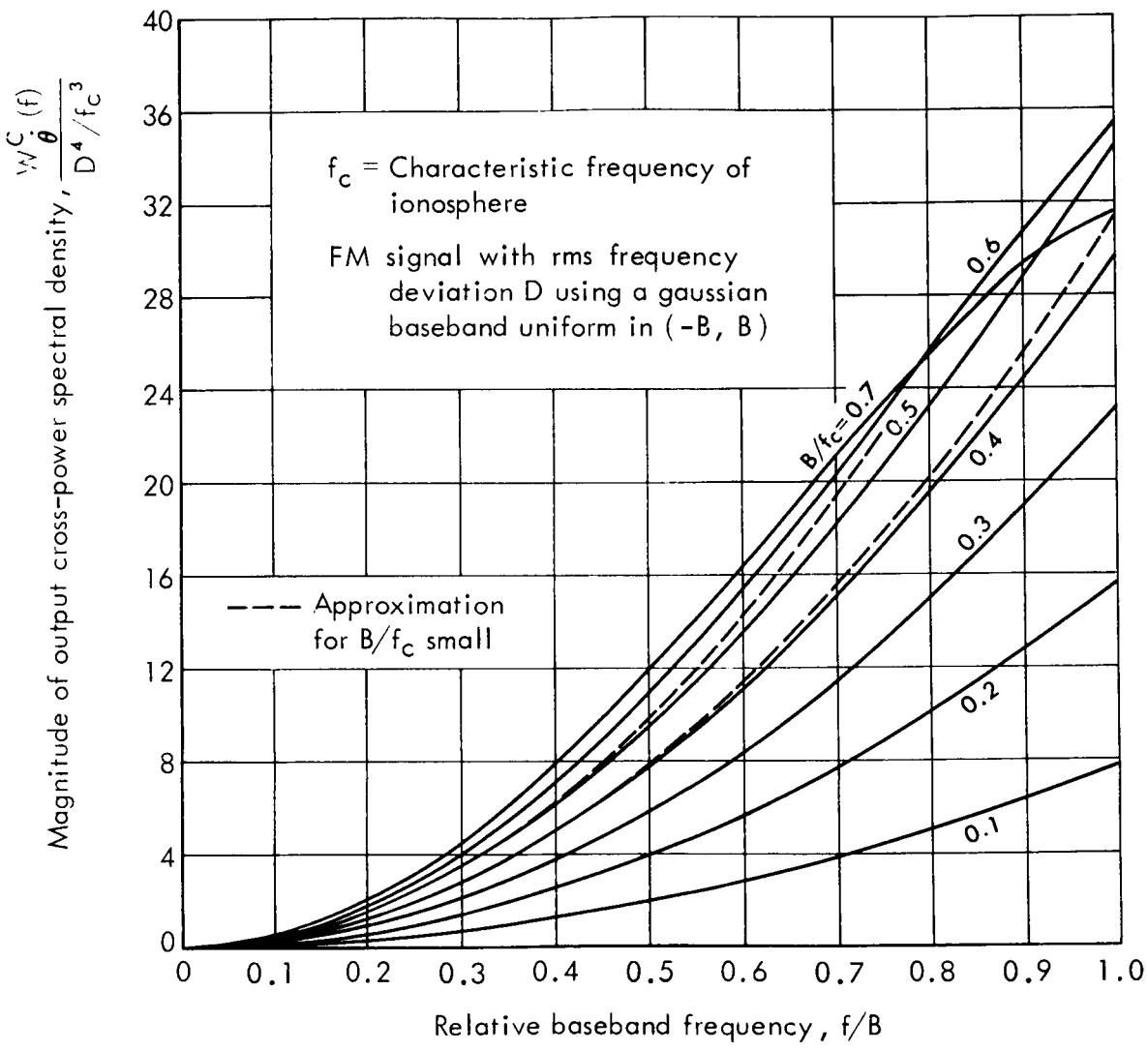

Fig. 4 — Magnitude of output cross-power spectral density
(Note that $W_{\dot\theta}^{c}$ is negative in this example.)

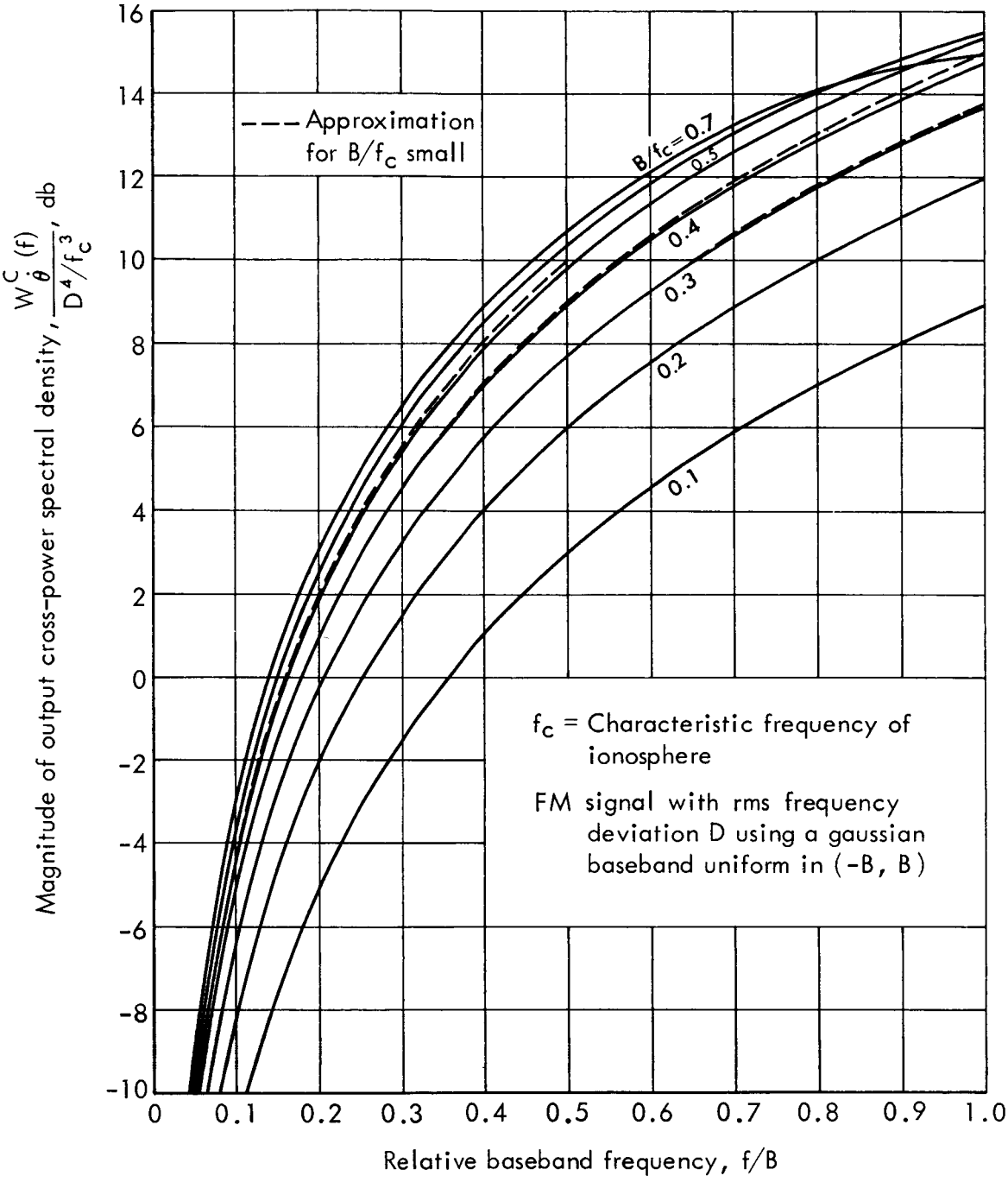

Fig.5—Magnitude of output cross-power spectral density, db, (Note that $W_{\dot\theta}^{c}$ is negative in this example.)

the cross-power stems from a cross-correlation and need not be so constrained. In this case, the spectrum is real and even but negative, at least for the range considered for the parameters. Other than that, the principal distinguishing feature of the cross-power spectral density is that it generally increases steadily across the baseband.

The intermodulation spectral density given by the third of Eqs. (35) is plotted in Figs. 6 and 7. Since the intermodulation is derived from an autocorrelation function, it too is a real, positive even function. As is characteristic of a second-order spectral density, it extends to twice the highest baseband frequency, falling smoothly to zero. Like the cross-power, the intermodulation increases across the baseband. Since the linear-signal is roughly constant, it follows that the cross-correlation between the intermodulation and the linear-signal, as indicated by the cross-power, is approximately constant across the baseband.

Narrow-band approximations to these spectra are readily obtained by expanding the circular functions in Eqs. (35) and retaining only the leading terms. Then,

$$\frac{W_{\dot{\theta}}^{L}(f)}{D^2/f_c} \cong \frac{2\pi^2}{\underline{B}} , \qquad |f| \le B$$

$$\frac{W_{\dot{\theta}}^{C}(f)}{D^4/f_c^3} \cong -\frac{8\pi^2}{\underline{B}} \underline{f}^2 , \qquad |f| \le B$$

$$\frac{W_{\dot{\theta}}^{I}(f)}{D^4/f_c^3} \cong \frac{2\pi^2}{\underline{B}^2} \underline{f}^2(2\underline{B}-|\underline{f}|) , \qquad |f| \le 2B \tag{36}$$

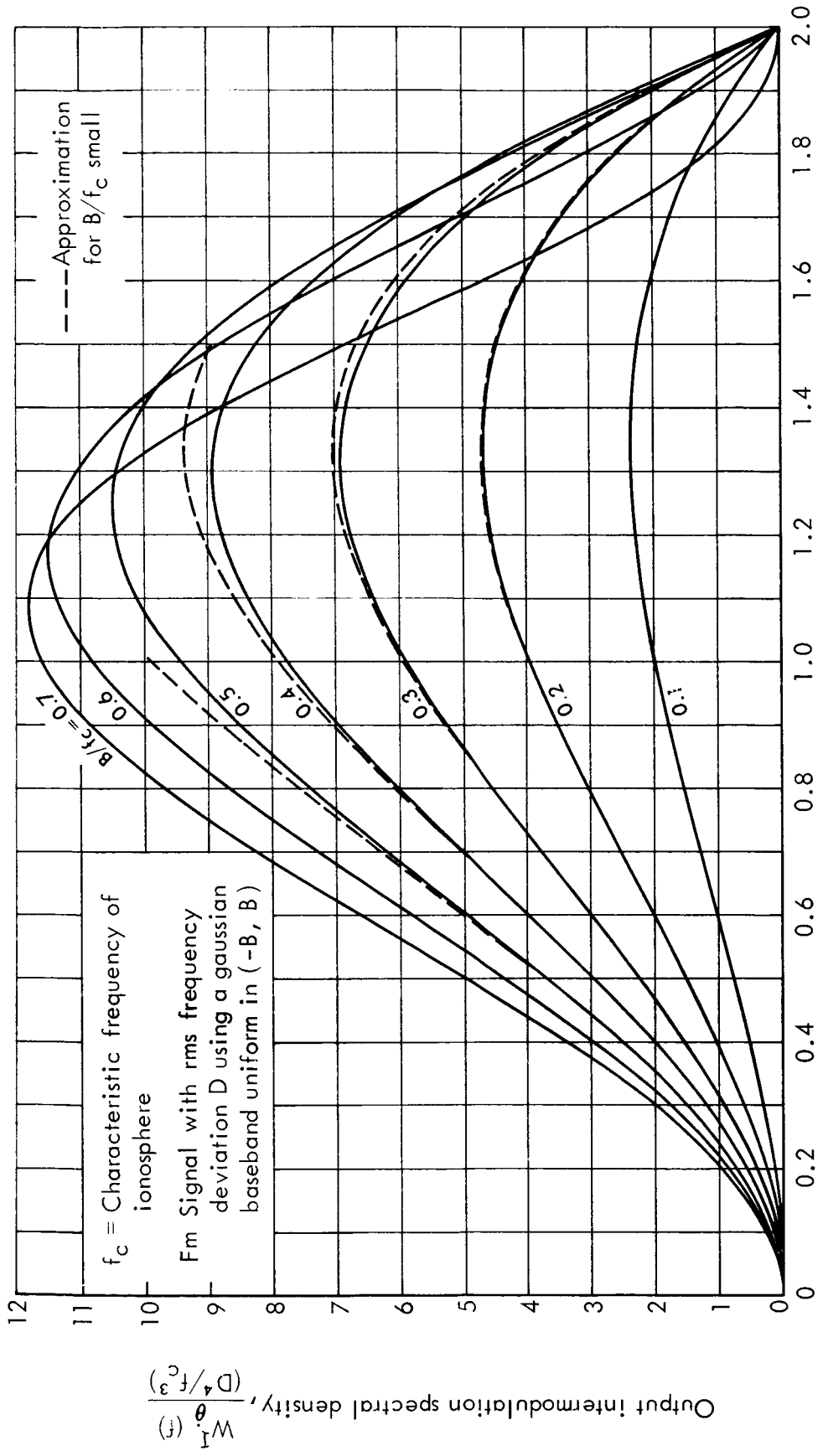

Fig. 6 — Output intermodulation spectral density

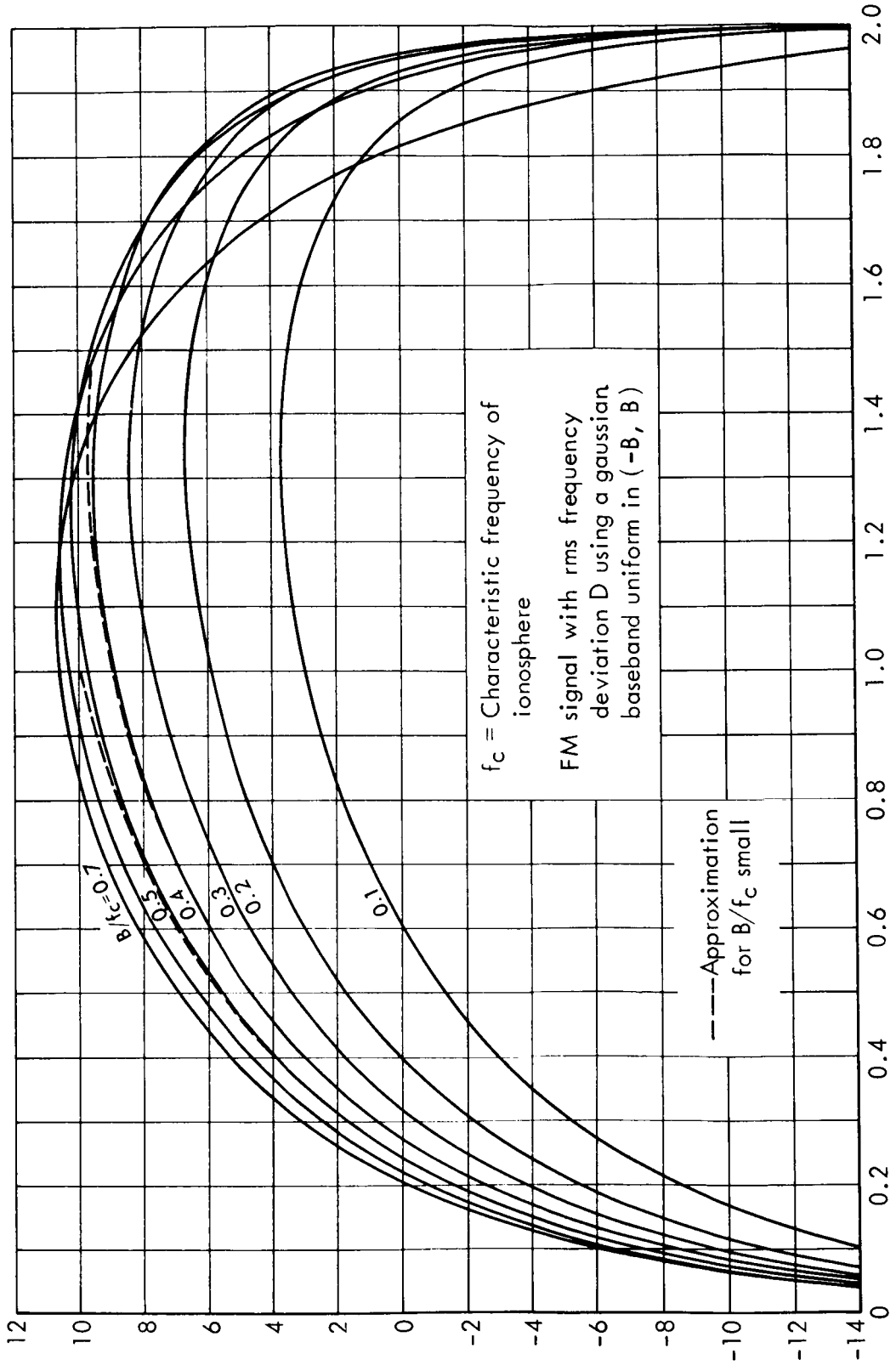

Fig. 7 — Output intermodulation spectral density, db

These spectra are plotted as dashed lines in Figs. 4 to 7 for the lower values of B/f_c. The results by Rice, Shaft, Prosin, and Denton, et al., mentioned in the Introduction, agree with the third of Eqs. (36) above. As seen in Figs. 4 to 7, the approximation is quite good for values of B/f_c up to about 0.5.

The ratio of the linear-signal to the intermodulation spectral densities, i.e., the ratio of the first and third of Eqs. (35), is plotted in Fig. 8. As explained in Ref. 6, this ratio approximates the signal-to-cross-talk ratio in a given channel of a multichannel, frequency-division-multiplexed modulating signal as a function of its position within the baseband. The approximation improves as the number of channels is increased. The poorest channel (i.e., the one with the lowest signal-to-cross-talk ratio) lies at the upper end of the baseband, a fact which compounds its difficulties since it is also the channel with the lowest signal-to-noise ratio due to thermal noise in the r-f channel.

Also shown in Fig. 8, as a dashed line, is the approximation available by forming the ratio of the first and third of Eqs. (36), i.e.,

$$\frac{W_{\dot{\theta}}^{I}(f)}{W_{\dot{\theta}}^{I}(f)} \times \frac{D^2}{f_c^2} \cong \frac{\underline{B}}{\underline{f}^2(2\underline{B}-|f|)}, \qquad |f| \leq B \tag{37}$$

To this approximation, the signal-to-cross-talk ratio, SCR, in the poorest channel is given by

$$SCR_{min} \cong \frac{W_{\dot{\theta}}^{L}(f)}{W_{\dot{\theta}}^{I}(f)} \cong \frac{1}{\underline{D}^2\underline{B}^2} \tag{38}$$

which is obtained by evaluating Eq. (37) at $|f| = B$.

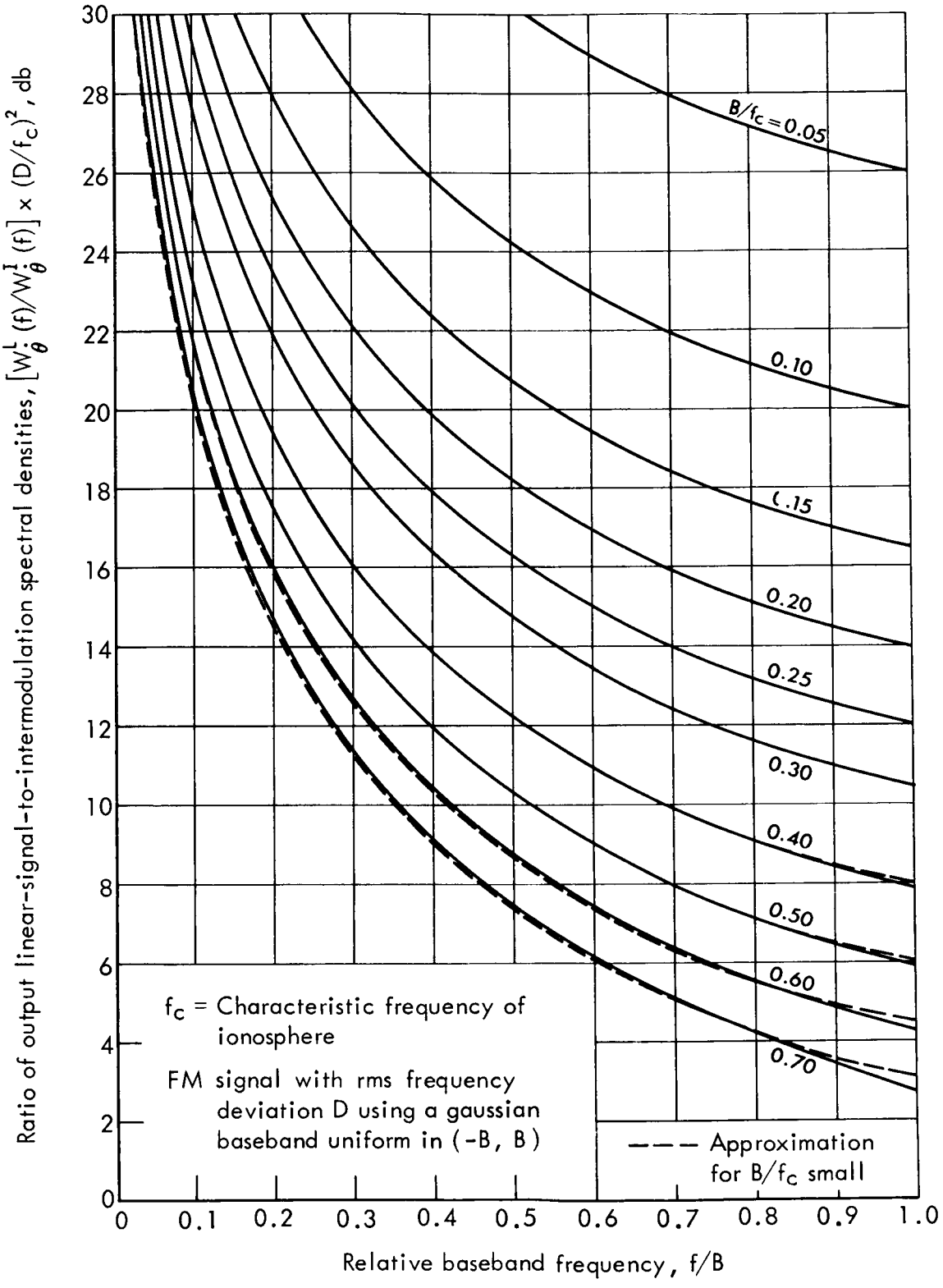

Fig.8—Ratio of output linear-signal-to-intermodulation spectral densities, db. This ratio approximates the signal-to-cross-talk ratio in a narrow channel as a function of its location within the baseband

The signal-to-distortion ratio, SDR, is the ratio of the total linear-signal to total intermodulation obtained by integrating the first and third of Eqs. (35) across the baseband and forming their ratio, which is plotted in Fig. 9. Again, an approximation can be obtained from Eqs. (36) yielding

$$\mathrm{SDR} \cong \frac{12}{5\,\underline{D}^2\underline{B}^2} \tag{39}$$

which is plotted as a dashed line in Fig. 9. Both the signal-to-cross-talk and the signal-to-distortion ratios are seen to be very well approximated by Eqs. (37) and (39) for the range of the baseband-to-characteristic frequency ratio, B/f_c, considered.

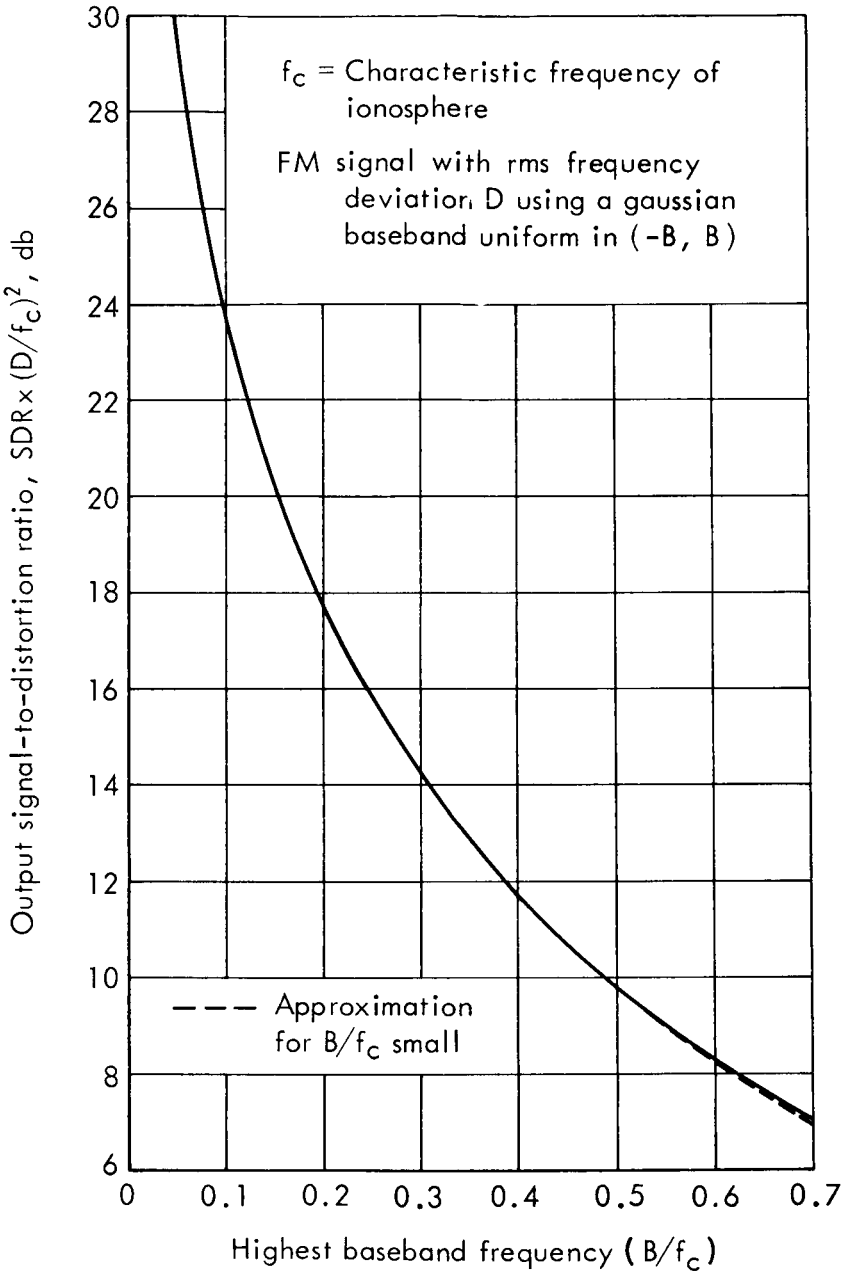

Fig. 9 — Output signal-to-distortion ratio in total baseband, db

VI. EXAMPLES AND DISCUSSION

The foregoing results can be applied to the problem of linking a terrestrial station to an earth satellite at synchronous altitude. The propagation path traverses virtually the entire ionosphere in a direction which depends on the relative location of the station and the satellite and can range from the zenith to the near-horizon. The integrated electron density, N_T, in Eq. (32) for a path to the zenith at midlatitudes through an average ionosphere amounts to about 10^{17} electrons/m^2, but can vary by a factor of 10 either way depending on the time of day, the season, the position in the solar cycle, and the geographical location.[8,9] Similarly, a path near the horizon can yield a value for N_T of from 10^{18} to 10^{19} electrons/m^2 under adverse conditions.

As an example of a particular application, consider a heavily trafficked point-to-point communication link via a synchronous earth satellite. Assume the down-link consists of a wide-band, FM transmission at a carrier frequency, f_o, of 4 GHz having an rms frequency deviation, D, of 20 MHz and using a CCIF standardized, 960-channel baseband which extends to a maximum baseband frequency, B, of 4.028 MHz. A worst-case ionospheric path having an integrated electron density of 10^{19} electrons/m^2 then yields a characteristic frequency, f_c, of 87 MHz from Fig. 1 or Eq. (33). The normalized maximum baseband frequency, $\underline{B}$, becomes 0.0463, and the normalized rms frequency deviation, $\underline{D}$, becomes 0.230, so from Eq. (38), the signal-to-cross-talk ratio, SCR_{min}, in the worst channel becomes 8830 (39.5 db).

This example indicates that ionospheric dispersion will not cause significant intermodulation distortion in a typical wide-band, FM,

communication-satellite link except under only the most severe, and, therefore, generally infrequent, conditions. The direct dependence of SCR_{min} on the various communication parameters is shown by combining Eqs. (33) and (38),

$$SCR_{min} = 1.401 \times 10^{12} \frac{f_o^6}{D^2 B^2 N_T^2} \tag{40}$$

The sixth-power dependence on carrier frequency clearly dominates. For example, f_o need only be halved (-18 db) to virtually overcome the effect of a tenfold decrease in N_T(-20 db). For a given baseband signal and r-f bandwidth, operation over a given path should be at as high a carrier frequency as possible.

Another example is the use of a satellite to relay TV programs (in color or monochrome) either directly to a viewer or to an intermediate station for conventional rebroadcast. Again, assume wide-band FM, but now with a carrier frequency, f_o, of 1 GHz and an rms frequency deviation, D, of 8 MHz (corresponding to an r-f channel about 50 MHz in width). The highest baseband frequency, B, for the 525-line video used in the United States is 4.5 MHz. Let the integrated electron density, N_T, be 4×10^{18} electrons/m^2 on the basis that transmissions in such a broadcast or relay mode will be confined to well-defined geographical locations and therefore be well above the horizon. In this case, the characteristic frequency, f_c, 17.2 MHz and the normalized parameters, $\underline{B}$ and $\underline{D}$, are, respectively, 0.262 and 0.465. Then, from Eq. (39), the output signal-to-distortion ratio, SDR, becomes 162 (22.1 db). Alternatively, from Fig. 9, SDR = 15.5 + 2 x 3.32 = 22.1 db, since $\underline{D}$ = 0.465 (-3.32 db).

Unfortunately, it is difficult to equate the subjective effect of this signal-to-distortion ratio in the output of an ionospherically dispersed FM transmission with that of a similar signal-to-noise ratio in the output of a conventional vestigial-sideband AM transmission corrupted by thermal noise. For one thing, the spectral density of thermal noise in the video is uniform for the AM transmission, whereas that of the intermodulation in the FM transmission goes roughly as the square of the baseband frequency. Thus, one might expect a greater effect on the high-frequency video content than on the low frequency video content. Also, thermal noise is generally uncorrelated with the signal whereas the intermodulation can display a strong correlation as evidenced by the magnitude of the cross-power spectral density. Therefore, the intermodulation can be expected to differ in appearance and subjective effect from the customary "snow."

Other aspects, unique to a video signal, must also be considered. One is the possibility that the intermodulation may affect the sound subcarrier, which is located above the video at 4.5 MHz. Although the intermodulation spectrum is at its strongest there, the sound subcarrier is relatively strong (a minimum of 50 percent of the peak picture power) and uses FM with a peak frequency deviation of only 25 kHz. These factors, plus the known superior coverage of the sound portion of conventional TV broadcast compared with the picture, suggest that this source of interference will probably not be significant.

The situation is less promising with respect to color TV. The color subcarrier is at 3.58 MHz with its attendant sidebands extending from roughly 2.5 to 4.5 MHz, again in the vicinity of the peak of the intermodulation spectral density. As a result, two effects can be

anticipated. First, the ratio of the linear-signal-to-intermodulation spectral density at which the color information must be demodulated (corresponding to the signal-to-cross-talk ratio in the previous example) will be unfavorable, amounting to about 18 or 19 db for this case. As a result, the color quality will be degraded much as it would be by thermal noise of comparable magnitude.

Second, the intermodulation can be expected to interfere with the synchronization of the color subcarrier generated in the receiver. The color subcarrier is suppressed at the transmitter and only short bursts (8 cycles of 3.58 MHz) are sent at the beginning of each horizontal line (i.e., at a 15,750 Hz rate). Because quadrature modulation is employed, the reference oscillator must be synchronized accurately in phase as well as frequency. Thus, intermodulation can degrade color separation by causing synchronizing phase errors.

It is likely that the subjective effect of ionospheric dispersion on a multichannel telephone trunk, as discussed above, can be estimated with a fair degree of accuracy using the numerical values computed by the theory presented here. However, such is probably not the case with respect to TV, particularly with color TV. The computations yield numbers, which, if interpreted as corresponding to interference produced by thermal noise, would be cause for concern. Whether the interference caused by ionospheric dispersion will be more or less objectionable in comparison is presently a matter of speculation and will probably remain so until experimental tests are conducted.

Appendix

SPECTRAL ANALYSIS

Let the output phase function given by Eq. (18) be written

$$\theta(t) = \beta + \Phi + f_2 + f_3 + \ldots \tag{A-1}$$

as suggested in Section III. Substituting into Eq. (19) for W_θ and expanding the result yields the variety of pairings of the $\Phi \times f$ form defined by Eq. (22). These will be examined in turn to obtain the various components of the output phase spectral density, W_θ.

$\beta \times \beta$

This first pairing immediately yields

$$\beta \times \beta = \beta_o^2 \, \delta(f) \tag{A-2}$$

where the expected value is a constant and the Fourier transform of a constant is a delta function at zero frequency, i.e., a dc term. The coefficient is given as the leading dc term in the first of Eqs. (23).

$\Phi \times \Phi$

This pairing can also be written directly by noting from Eq. (17) that Φ_r is the response when φ is applied to a filter having an impulse response, γ_r. The associated steady-state transfer is seen, from Eqs. (13), to be Δ so

$$\Phi \times \Phi = |\Delta(f)|^2 W_\varphi(f) \tag{A-3}$$

By definition, this is the linear-signal component of W_θ and is the second of Eqs. (23).

$\underline{\beta \times f_2}$

There are two terms of this type in Eq. (19), but they are equivalent since β is not a function of time. Thus, from Eq. (18),

$$\beta \times f_2 = 2(-\beta_o)(-)\frac{1}{2}\,\Im \int_0^\infty \gamma_i(\mu) E[\varphi(t-u)-\Phi_r(t)]^2 du \tag{A-4}$$

The expected value in Eq. (A-4) has been computed previously and is given by Eq. (C-12) of Ref. 10; viz.,

$$E[\varphi(t-u)-\Phi_r(t)]^2 = \int_{-\infty}^{\infty} d\rho\; W_\varphi(\rho)\left[|\Delta(\rho)|^2 - 2\,\Delta(\rho)e^{i2\pi\rho\mu} + 1\right] \tag{A-5}$$

Performing the integration on μ then yields

$$\beta \times f_2 = -\,2\beta_o\,\Im \int_{-\infty}^{\infty} d\rho\; W_\varphi(\rho)\Delta(\rho)\Lambda(-\rho) \tag{A-6}$$

where the first and third terms in Eq. (A-5) have disappeared by virtue of the second of Eqs. (12). The functions Δ and Λ are identified from Eqs. (13).

As with Eq. (A-2), the Fourier transform yields a delta function at zero frequency. Also, the fact that W_φ is an even function can be used to write

$$\begin{aligned}
\beta \times f_2 &= -\,\beta_o\delta(f) \int_{-\infty}^{\infty} d\rho\; W_\varphi(\rho)\left[\Delta(\rho)\Lambda(-\rho)+\Delta(-\rho)\Lambda(-\rho)\right] \\
&= -\,\beta_o\delta(f) \int_{-\infty}^{\infty} d\rho\; W_\varphi(\rho)\left[\Delta(\rho)\Lambda(-\rho)+\Delta^*(\rho)\Lambda^*(-\rho)\right] \\
&= -\,2\beta_o\delta(f) \int_{-\infty}^{0} d\rho\; W_\varphi(\rho)\,\mathrm{Re}\;\Delta(\rho)\Lambda(-\rho)
\end{aligned} \tag{A-7}$$

where the symmetry properties of Δ and Λ given by Eqs. (15) have been employed. The coefficient of δ above is given as the second-order dc term in the first of Eqs. (23).

The computation of the higher order terms requires evaluating the expected value of fourth-order products of the gaussian variates. Two of the methods available have been used in previous reports. In one of these, the desired expected value is identified as the coefficient of the appropriate term in the expansion of the expected value of a specially constructed exponential function, details are given in Appendix B of Ref. 6. The other method uses the relation

$$E(x_1 x_2 \ldots x_{2n}) = \sum_{\text{all pairs}} E(x,x;)E(x_j x_k) \ldots E(x_\ell x_{2n}) \qquad \text{(A-8)}$$

as described in Appendix C of Ref. 10, which is used here.

$\Phi \times f_3$

There are two terms of this type in Eq. (19), i.e.,

$$\begin{aligned} \Phi \times f_3 &= \Im\, E[\Phi(t) f_3(t+\tau) + \Phi(t+\tau) f_3(t)] \\ &= \Im\, E[\Phi(t-\tau) f_3(t) + \Phi(t+\tau) f_3(t)] \end{aligned} \qquad \text{(A-9)}$$

Since the terms in Eq. (A-9) differ only in the sign of τ, they will simply be written singly with a $\pm$ notation, the sum being understood. Then, from Eq. (18),

$$\begin{aligned} \Phi \times f_3 = \Im\, E \Big\{ &- \frac{1}{6} \Phi_r(t \pm \tau) \int_0^\infty \gamma_r(x)[\varphi(t-x) - \Phi_r(t)]^3 dr \\ &- \frac{1}{2} \Phi_r(t \pm \tau) \Phi_i(t) \int_0^\infty \gamma_i(x)[\varphi(t-x) - \Phi_r(t)]^2 dx \Big\} \end{aligned} \qquad \text{(A-10)}$$

The term in the upper line of Eq. (A-10) is identical in form to Eq. (C-4) of Ref. 10. Its value is given by Eq. (C-18) of Ref. 10 as

$$2\, W_\varphi(f) \int_{-\infty}^{\infty} d\rho\; W_\varphi(\rho) \left\{ \mathrm{Re}\; \Delta(\rho)\Delta(-\rho-f)\Delta(f) - |\Delta(f)|^2 |\Delta(\rho)|^2 \right\} \tag{A-11}$$

The other term in Eq. (A-10) remains to be computed. Using Eq. (17) to expand the initial Φ's yields

$$-\frac{1}{2} \int_0^{\infty} du \int_0^{\infty} dv \int_0^{\infty} dw\; \gamma_r(u)\gamma_i(v)\gamma_i(w)$$

$$\Im\, E\, \varphi(t\pm\tau-u)\varphi(t-v)[\varphi(t-w) - \Phi_r(t)]^2 \tag{A-12}$$

According to Eq. (A-8), the expected values in this expression can be expanded in the form

$$E(abc^2) = E(ab)E(c^2) + 2E(ac)E(bc) \tag{A-13}$$

The various expected values are

$$E(ab) = E\, \varphi(t\pm\tau-u)\varphi(t-v)$$

$$= R_\varphi(\pm\tau-u+v) \tag{A-14}$$

where the autocorrelation function in Eq. (20) has been used,

$$E(c^2) = E[\varphi(t-w) - \Phi_r(t)]^2$$

$$= \int_{-\infty}^{\infty} d\rho\; W_\varphi(\rho)\left[|\Delta(\rho)|^2 - 2\Delta(\rho)e^{i2\pi\rho w} + 1\right] \tag{A-15}$$

which follows from Eq. (A-5),

$$E(ac) = E\,\varphi(t\pm\tau-u)\,[\varphi(t-w) - \Phi_r(t)]$$

$$= R_\varphi(\pm\tau-u+w) - \int_0^\infty dx\ \gamma_r(x) R_\varphi(\pm\tau-u+x) \qquad \text{(A-16)}$$

$$E(bc) = E\,\varphi(t-v)\,[\varphi(t-w) - \Phi_r(t)]$$

$$= R_\varphi(v-w) - \int_0^\infty dx\ \gamma_r(x) R_\varphi(v-x)$$

$$= \int_{-\infty}^{\infty} d\rho\ W_\varphi(\rho) e^{i2\pi\rho(v-w)} - \int_0^\infty dx\ \gamma_r(x) \int_{-\infty}^{\infty} d\rho\ W_\varphi(\rho) e^{i2\pi\rho(v-x)}$$

$$= \int_{-\infty}^{\infty} d\rho\ W_\varphi(\rho) e^{i2\pi\rho v} \left[e^{-i2\pi\rho w} - \Delta(\rho)\right] \qquad \text{(A-17)}$$

The Fourier transforms of Eqs. (A-14) and (A-16) are

$$\mathfrak{F}\,E(ab) = \int_{-\infty}^{\infty} d\tau\ e^{-i2\pi f\tau}\ R_\varphi(\pm\tau-u+v)$$

$$= e^{\mp i2\pi f(u-v)}\ W_\varphi(f) \qquad \text{(A-18)}$$

$$\mathfrak{F}\,E(ac) = \int_{-\infty}^{\infty} d\tau\ e^{-i2\pi f\tau} \left[R_\varphi(\pm\tau-u+w) - \int_0^\infty dx\ \gamma_r(x) R_\varphi(\pm\tau-u+x)\right]$$

$$= e^{\mp i2\pi f(u-w)}\ W_\varphi(f) - e^{\mp i2\pi fu}\ \Delta(\mp f) W_\varphi(f)$$

$$= e^{\mp i2\pi fu}\ W_\varphi(f) \left[e^{\pm i2\pi fw} - \Delta(\mp f)\right] \qquad \text{(A-19)}$$

Combining Eqs. (A-15), (A-17)-(A-19) in Eq. (A-13) yields

$$\mathfrak{F}\, E(abc^2) = E(c^2)\mathfrak{F}\, E(ab) + 2E(bc)\mathfrak{F}\, E(ac)$$

$$= e^{\mp i2\pi fu} W_\varphi(f)\left\{e^{\pm i2\pi fv}\int_{-\infty}^{\infty} d\rho\; W_\varphi(\rho)\left[\,|\Delta(\rho)|^2 - 2\Delta(\rho)e^{i2\pi\rho w} + 1\right]\right.$$

$$\left. + 2\left[e^{\pm i2\pi fw} - \Delta(\mp f)\right]\int_{-\infty}^{\infty} d\rho\; W_\varphi(\rho)e^{i2\pi\rho v}\left[e^{-i2\pi\rho w} - \Delta(\rho)\right]\right\} \qquad \text{(A-20)}$$

When substituted into expression (A-12), the integration on u follows immediately, resulting in

$$-\frac{1}{2}\,\Delta(\pm f)W_\varphi(f)\int_0^\infty dv\int_0^\infty dw\;\gamma_i(v)\gamma_i(w) \quad \left\{\begin{matrix}\text{term in braces}\\ \text{in Eq. (A-20)}\end{matrix}\right\} \qquad \text{(A-21)}$$

Integrating on v further yields

$$-\frac{1}{2}\,\Delta(\pm f)W_\varphi(f)\int_0^\infty dw\;\gamma_i(w)$$

$$\left\{\Lambda(\mp f)\int_{-\infty}^{\infty} d\rho\; W_\varphi(\rho)\left[\,|\Delta(\rho)|^2 - \Delta(\rho)e^{i2\pi\rho w} + 1\right]\right.$$

$$\left. + 2\left[e^{\pm i2\pi fw} - \Delta(\mp f)\right]\int_{-\infty}^{\infty} d\rho\; W_\varphi(\rho)\Lambda(-\rho)\left[e^{-i2\pi\rho w} - \Delta(\rho)\right]\right\}$$

$$= -\frac{1}{2}\,\Delta(\pm f)W_\varphi(f)\int_{-\infty}^{\infty} d\rho\; W_\varphi(\rho)\int_0^\infty dw\;\gamma_i(w)$$

$$\left\{\Lambda(\mp f)\left[\,|\Delta(\rho)|^2 - 2\Delta(\rho)e^{i2\pi\rho w} + 1\right]\right.$$

$$\left. + 2\Lambda(-\rho)\left[e^{\pm i2\pi fw} - \Delta(\mp f)\right]\left[e^{-i2\pi\rho w} - \Delta(\rho)\right]\right\} \qquad \text{(A-22)}$$

The terms not involving the exponentials vanish when integrated on w, by virtue of the second of Eqs. (12), yielding

$$- \frac{1}{2}\,\Delta(\pm f)W_\varphi(f)\int_{-\infty}^{\infty} d\rho\; W_\varphi(\rho)\,\Big\{-2\Lambda(\mp f)\Delta(\rho)\Lambda(-\rho)$$

$$+\; 2\Lambda(-\rho)[\Lambda(\mp f+\rho)-\Delta(\mp f)\Lambda(\rho)-\Delta(\rho)\Lambda(\mp f)]\Big\}$$

$$= W_\varphi(f)\int_{-\infty}^{\infty} d\rho\; W_\varphi(\rho)\Delta(\pm f)[2\Lambda(\mp f)\Delta(\rho)\Lambda(-\rho)$$

$$-\; \Lambda(-\rho)\Lambda(\mp f+\rho)+\Lambda(-\rho)\Delta(\mp f)\Lambda(\rho)]$$

$$= W_\varphi(f)\int_{-\infty}^{\infty} d\rho\; W_\varphi(\rho)\,\Big\{\Delta(\pm f)\Lambda(-\rho)[2\Lambda(\mp f)\Delta(\rho)-\Lambda(\mp f+\rho)]$$

$$+\; |\Delta(\pm f)|^2|\Lambda(\rho)|^2\Big\} \qquad \text{(A-23)}$$

where the symmetry properties of Δ and Λ given by Eqs. (15) have been used in the last step. Dropping the $\pm$ notation and writing expression (A-23) as a sum yields

$$W_\varphi(f)\int_{-\infty}^{\infty} d\rho\; W_\varphi(\rho)[2\Delta(f)\Lambda(-\rho)\Lambda(-f)\Delta(\rho) - \Delta(f)\Lambda(-\rho)\Lambda(-f+\rho)$$

$$+\; |\Delta(f)|^2|\Lambda(\rho)|^2 + 2\Delta(-f)\Lambda(-\rho)\Lambda(f)\Delta(\rho)$$

$$-\; \Delta(-f)\Lambda(-\rho)\Lambda(f+\rho) + |\Delta(-f)|^2|\Lambda(\rho)|^2\,] \qquad \text{(A-24)}$$

Changing the sign of the variable, ρ, in the second and third terms results in

$$W_\varphi(f)\int_{-\infty}^{\infty} d\rho\; W_\varphi(\rho)[2\Delta(f)\Lambda(-\rho)\Lambda(-f)\Delta(\rho) - \Delta(f)\Lambda(\rho)\Lambda(-f-\rho)$$

$$+\; 2\Delta(-f)\Lambda(\rho)\Lambda(f)\Delta(-\rho) - \Delta(-f)\Lambda(\rho)\Lambda(f+\rho) + 2|\Delta(f)|^2|\Lambda(\rho)|^2]$$

$$= 2W_\varphi(f)\int_{-\infty}^{\infty} d\rho\; W_\varphi(\rho)[2\ \mathrm{Re}\ \Delta(f)\Lambda(-\rho)\Lambda(-f)\Delta(\rho) - \mathrm{Re}\ \Delta(f)\Lambda(\rho)\Lambda(-f-\rho)$$

$$+\; 2|\Delta(f)|^2|\Lambda(\rho)|^2\,] \qquad \text{(A-25)}$$

where the symmetry properties of Δ and Λ have again been used.

The total $\Phi \times f_3$ is the sum of expressions (A-11) and (A-25),

$$\Phi \times f_3 = 2W_\varphi(f) \int_{-\infty}^{\infty} d\rho \; W_\varphi(\rho) \left\{ \mathrm{Re}\, \Delta(f)[\Delta(\rho)\Delta(-\rho-f) - \Lambda(\rho)\Lambda(-f-\rho)] \right.$$

$$\left. + |\Delta(f)|^2[|\Lambda(\rho)|^2 - |\Delta(\rho)|^2] + 2\mathrm{Re}\, \Delta(f)\Lambda(-f)\Delta(\rho)\Lambda(-\rho) \right\} \qquad \text{(A-26)}$$

This contribution is the leading cross-power term and is listed as the third of Eqs. (23)

$\underline{f_2 \times f_2}$

From Eq. (18), this term is

$$f_2 \times f_2 = \frac{1}{4} \int_0^{\infty} du \; \gamma_i(u) \int_0^{\infty} dv \; \gamma_i(v)$$

$$\mathfrak{F}\, E\left\{ [\varphi(t-u) - \Phi_r(t)]^2 [\varphi(t+\tau-v) - \Phi_r(t+\tau)]^2 \right\} \qquad \text{(A-27)}$$

Expanding the expected value according to Eq. (A-8) yields

$$E(a^2b^2) = E(a^2)E(b^2) + 2E^2(ab) \qquad \text{(A-28)}$$

The expected values

$$E(a^2) = E[\varphi(t-u) - \Phi_r(t)]^2$$

$$E(b^2) = E[\varphi(t+\tau-v) - \Phi_r(t+\tau)]^2 \qquad \text{(A-29)}$$

are equivalent and are both given by Eq. (A-15). Since the variable τ disappears on applying the expectation operator, taking the Fourier transform results in a zero-frequency delta function. Thus, the contribution of this term to Eq. (A-27) is

$$\frac{1}{4}\delta(f) \int_0^{\infty} du \; \gamma_i(u) \int_0^{\infty} dv \; \gamma_i(v) \int_{-\infty}^{\infty} d\rho \; W_\varphi(\rho) \int_{-\infty}^{\infty} d\sigma \; W_\varphi(\sigma)$$

$$[|\Delta(\rho)|^2 - 2\Delta(\rho)e^{i2\pi\rho u} + 1]\; [|\Delta(\sigma)|^2 - 2\Delta(\sigma)e^{i2\pi\rho v} + 1] \qquad \text{(A-30)}$$

Again by virtue of the second of Eqs. (12), only the terms involving the appropriate exponentials remain when the integrations on u and v are performed. The result is

$$\delta(f)\Big[\int_{-\infty}^{\infty} d\rho\ W_\varphi(\rho)\Delta(\rho)\Lambda(-\rho)\Big]\Big[\int_{-\infty}^{\infty} d\sigma\ W_\varphi(\sigma)\Delta(\sigma)\Lambda(-\sigma)\Big]$$

$$= \delta(f)\Big[\int_{-\infty}^{\infty} d\rho\ W_\varphi(\rho)\,\mathrm{Re}\ \Delta(\rho)\Lambda(-\rho)\Big]^2 \qquad \text{(A-31)}$$

where the symmetry properties of Δ and Λ are again used. This term is not listed in Eqs. (23), since it is clearly a third-order dc term (another contribution of the same order can be expected from the $\beta \times f_4$ term).

The expected value in the second term of Eq. (A-28) is similar in form to Eq. (C-26) of Ref. 10,

$$E(ab) = \int_{-\infty}^{\infty} d\rho\ W_\varphi(\rho)e^{i2\pi\rho\tau}\Big[\Delta(\rho)-e^{-i2\pi\rho v}\Big]\Big[\Delta(-\rho)-e^{i2\pi\rho u}\Big] \qquad \text{(A-32)}$$

Substituting first into Eq. (A-28) and then into Eq. (A-27) yields

$$\frac{1}{2}\int_0^{\infty} du \int_0^{\infty} dv\ \gamma_i(u)\gamma_i(v)$$

$$\Im\Big\{\int_{-\infty}^{\infty} d\rho\ W_\varphi(\rho)e^{i2\pi\rho\tau}\Big[\Delta(\rho)-e^{-i2\pi\rho v}\Big]\Big[\Delta(-\rho)-e^{i2\pi\rho u}\Big]$$

$$\int_{-\infty}^{\infty} d\sigma\ W_\varphi(\sigma)e^{i2\pi\sigma\tau}\Big[\Delta(\sigma)-e^{-i2\pi\sigma v}\Big]\Big[\Delta(-\sigma)-e^{i2\pi\sigma u}\Big]\Big\}$$

$$= \frac{1}{2}\int_{-\infty}^{\infty} d\rho \int_{-\infty}^{\infty} d\sigma\ W_\varphi(\rho)W_\varphi(\sigma)\Im\ e^{i2\pi(\rho+\sigma)\tau}$$

$$\Big\{\int_0^{\infty} du\ \gamma_i(u)\Big[\Delta(-\rho)-e^{i2\pi\rho u}\Big]\Big[\Delta(-\sigma)-e^{i2\pi\sigma u}\Big]$$

$$\int_0^{\infty} dv\ \gamma_i(v)\Big[\Delta(\rho)-e^{-i2\pi\rho v}\Big]\Big[\Delta(\sigma)-e^{-i2\pi\sigma v}\Big]\Big\} \qquad \text{(A-33)}$$

The integral on u in the second line is evaluated by expanding the integrand and integrating term by term

$$\int_0^\infty du\ \gamma_i(u)\ \left[\Delta(-\rho)\Delta(-\sigma)-\Delta(-\sigma)e^{i2\pi\rho u}-\Delta(-\rho)e^{i2\pi\sigma u}+e^{i2\pi(\rho+\sigma)u}\right]$$

$$= -\Delta(-\sigma)\Lambda(-\rho)-\Delta(-\rho)\Lambda(-\sigma)+\Lambda(-\rho-\sigma) \qquad \text{(A-34)}$$

Analogously, the integral on v in the third line is

$$-\Delta(\sigma)\Lambda(\rho)\ -\ \Delta(\rho)\Lambda(\sigma)\ +\ \Lambda(\rho+\sigma) \qquad \text{(A-35)}$$

The product of these expressions, which are complex conjugates, is simply the square of their magnitude. Substituting in (A-33), taking the Fourier transform and integrating on σ yields

$$\frac{1}{2}\int_{-\infty}^{\infty} d\rho \int_{-\infty}^{\infty} d\sigma\ W_\varphi(\rho)W_\varphi(\sigma)\delta(f-\rho-\sigma)$$

$$\left|\Delta(\rho)\Lambda(\sigma)\ +\ \Lambda(\rho)\Delta(\sigma)\ -\ \Lambda(\rho+\sigma)\right|^2$$

$$= \frac{1}{2}\int_{-\infty}^{\infty} d\rho\ W_\varphi(\rho)W_\varphi(f-\rho)\left|\Delta(\rho)\Lambda(f-\rho)+\Lambda(\rho)\Delta(f-\rho)-\Lambda(f)\right|^2 \qquad \text{(A-36)}$$

which is the leading intermodulation component and is listed as the last of Eqs. (23).

REFERENCES

1. Bedrosian, E., et al., Multiple Access Techniques for Communication Satellites: I. Survey of the Problem, The RAND Corporation, RM-4298-NASA, September 1964, pp. 70-75.

2. Rice, S. O., "Distortion Produced in a Noise Modulated FM Signal by Nonlinear Attenuation and Phase Shift," B.S.T.J., Vol. 36, No. 4, July 1957, pp. 879-890.

3. Shaft, P. D., "Distortion of Multitone FM Signals Due to Phase Nonlinearity," Trans. IEEE, Vol. SET-9, No. 1, March 1963, pp. 25-35.

4. Prosin, A. V., "Theory of Passing Wideband Signals in Earth-satellite Communications Systems," Radiotekhnika e Elektronica, Vol. 8, No. 11, 1963, pp. 1710-1720.

5. Denton, H., P. Scheibe, and J. Huntsberger, Dispersive Path Effects on Angle-modulated Signals, ESL Inc., ESL-IR9, October 20, 1965.

6. Bedrosian, E., and S. O. Rice, Distortion and Crosstalk of Linearly Filtered, Angle-modulated Signals, The RAND Corporation, P-3502, March 1967.

7. Stratton, J. A., Electromagnetic Theory, McGraw-Hill Book Company, New York, 1941, p. 327.

8. Lawrence, R. S., C. G. Little, and H. J. A. Chivers, "A Survey of Ionospheric Effects Upon Earth-space Radio Propagation," Proc. IEEE, Vol. 52, No. 1, January 1964, pp. 4-27.

9. Taylor, G. N., and G. H. Millman in Electron Density Profiles in Ionosphere and Exosphere, John Wiley and Sons, New York, 1966, pp. 543-548 and 555-566.

10. Bedrosian, E., Distortion and Crosstalk of Linearly Filtered, Angle-modulated Signals, The RAND Corporation, RM-4888-NASA, March 1966.